Ramp-induced transitions in traffic dynamics

Ding-wei Huang
Department of Physics, Chung Yuan Christian University, Chung-li, Taiwan
(Received 9 August 2005; published 19 January 2006)

We present the analytical results of ramp effects in asymmetric simple exclusion processes. Both on-ramp and off-ramp are included in between the two open boundaries. The ramps can be taken as the nontrivial boundaries to trigger the phase transitions. Exact phase diagrams are obtained analytically in the full parameter space. We find that the order of the two ramps is crucial. When the on-ramp is placed after the off-ramp along the traffic direction, there are only four distinct phases: free-free-free, free-free-jam, free-jam-jam, and jam-jam-jam. The other four phases from naive expectation cannot be realized, i.e., jam-free-free, jam-jam-free, jam-free-jam, and free-jam-free are all absent. The free flow will not follow the congestion. When the on-ramp is placed before the off-ramp, we observe an interesting phase: jam-max.-free. The bottleneck emerges as the flow in between the two ramps saturates to its maximum. We further show that the roadway configuration is equivalent to a nonstandard intersection. Applications to a traffic rotary are discussed.

DOI: 10.1103/PhysRevE.73.016123 PACS number(s): 89.40.−a, 64.60.Cn, 05.40.−a

I. INTRODUCTION

Recently, traffic-related problems have attracted much attention from physicists [1,2]. Not only are the problems highly relevant to our modern life, they also provide excellent examples to the phenomena of boundary-induced phase transitions [3,4]. Traffic flow is basically a one-dimensional phenomenon. From intuition, the congestion results whenever the in-flow is larger than the out-flow. On the other hand, if the in-flow is less than the out-flow, the vehicles might move freely. Such impressions are based on the perspective of transient situations. In practice, the free flow and/or congestion can be steady phases on the roadway. Such steady phases are present in a system driven far away from equilibrium, where a steady current is maintained asymptotically. The basic way to capture such a feature is the asymmetric simple exclusion processes [5,6]. The model has been studied thoroughly in a simple configuration of one roadway with two open ends and no ramp. The ramps can be thought of as nontrivial boundaries to influence the traffic greatly [7–9]. In a previous work [10], we studied the effects of a single ramp set up in between two open ends. The exact results were obtained analytically. In the presence of two ramps, only partial results were obtained. The two ramps were presumed to be operated at the same rate. In this work, we present the full results. The two ramps can be operated independently. We also introduce more ramps along the roadway and study their influence to the traffic. As a step towards the complex network, the flow around a traffic rotary is also analyzed. We emphasize that the exact phase diagrams are obtained. The full parameter space can be completely classified.

II. MODEL

We study the phase diagram of asymmetric simple exclusion processes with open boundaries and ramps. The system configurations are shown in Fig. 1. A simple roadway is represented by a one-dimensional lattice. Each site can be accommodated by one particle only. At each time step, every particle hops forward to the next site as long as that site is empty in previous time step. The dynamics in bulk is fully deterministic. There are four nontrivial sites: particles can be injected from the first site (left end) and from the site designated as the on-ramp; particles can also be removed from the last site (right end) and from the site designated as the off-ramp. Although particles move deterministically along the main road, their injection and removal from these four special sites are stochastic. The injection rates from the left end and the on-ramp are denoted by α_0 and α_1, respectively; the removal rates from the right end and the off-ramp are denoted by β_0 and β_1, respectively. On a homogeneous roadway, the traffic phase can be either free flow (F) or jam (J). These two phases can be distinguished by the bulk property and the boundary behavior. In the free flow, the traffic flow is proportional to the density. A flat density distribution can be observed except near the removal boundary, i.e., the injection boundary dictates the dynamics in bulk. In contrast, the flow decreases with the increase of density in the congestion. The removal boundary then dictates the bulk property and pro-

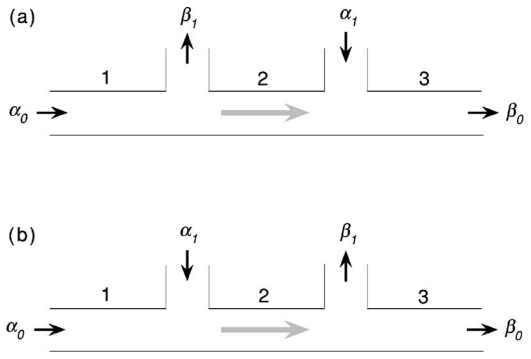

FIG. 1. System configurations: (a) on-ramp α_1 placed after off-ramp β_1 and (b) on-ramp α_1 placed before off-ramp β_1. The gray arrow shows the direction of particle hopping. The three parts of the roadway are labeled by the number. We note that changing the lengths of these three parts does not alter the phase diagrams to be shown later. Only the relative order of the ramps is relevant.

vides a nonflat profile near the injection boundary. It is interesting to note that the maximum flow (M) presents as the transition boundary between these two phases in extreme conditions. Only when there are at least two ramps properly situated can the maximum flow be supported as a distinct phase, where the bulk property becomes independent of boundaries.

In our previous study [10], we had obtained the analytical phase diagrams in the cases of a single ramp. The results can be summarized as follows.

With a single on-ramp ($\beta_1=0$), we have

$$\text{(F-F)} \quad \alpha_0 < \beta_0, \quad 0 < \alpha_1 < \frac{\beta_0 - \alpha_0}{1+\alpha_0}; \tag{1}$$

$$\text{(F-J)} \quad \alpha_0 < \beta_0, \quad \frac{\beta_0 - \alpha_0}{1+\alpha_0} < \alpha_1 < \frac{\beta_0 - \alpha_0}{\beta_0(1+\alpha_0)}; \tag{2}$$

$$\text{(J-J)} \quad \alpha_0 < \beta_0, \quad \frac{\beta_0 - \alpha_0}{\beta_0(1+\alpha_0)} < \alpha_1 < 1; \tag{3}$$

$$\text{or} \quad \beta_0 < \alpha_0, \quad 0 < \alpha_1 < 1. \tag{4}$$

The ramp divides the roadway into two parts. Each part can be taken effectively as a homogeneous roadway characterized by either free flow (F) or jam (J). When we start with a free-flow condition on the roadway ($\alpha_0 < \beta_0$) and then increase the ramp flow α_1, the free flow can be maintained at small α_1. As α_1 increases, the congestion begins to emerge in the second part of the roadway. Further increasing α_1 will bring the congestion into the first part of the roadway. If we start with the congestion on the roadway ($\beta_0 < \alpha_0$), any setting of α_1 will not resolve the traffic jams. In total, there are three distinct phases. The (J-F) phase cannot be realized.

In contrast, with a single off-ramp ($\alpha_1=0$), we have

$$\text{(J-J)} \quad \beta_0 < \alpha_0, \quad 0 < \beta_1 < \frac{\alpha_0 - \beta_0}{1+\beta_0}; \tag{5}$$

$$\text{(F-J)} \quad \beta_0 < \alpha_0, \quad \frac{\alpha_0 - \beta_0}{1+\beta_0} < \beta_1 < \frac{\alpha_0 - \beta_0}{\alpha_0(1+\beta_0)}; \tag{6}$$

$$\text{(F-F)} \quad \beta_0 < \alpha_0, \quad \frac{\alpha_0 - \beta_0}{\alpha_0(1+\beta_0)} < \beta_1 < 1; \tag{7}$$

$$\text{or} \quad \alpha_0 < \beta_0, \quad 0 < \beta_1 < 1. \tag{8}$$

As the ramp flow β_1 increases, the system will change from congestion to free flow. The same three phases are observed. It is interesting to note that the (J-F) phase is absent in both cases.

Now, we consider the case of two ramps, first with the off-ramp placed before the on-ramp as shown in Fig. 1(a). As the two ramps divide the roadway into three homogeneous parts, we can replace the ramp flow by effective boundaries. The flow through the off-ramp β_1 can be represented by a removal rate β' for the first part and an injection rate α' for the second part of the roadway; the flow through the on-ramp α_1 can also be represented by a removal rate β'' for the second part and an injection rate α'' for the third part of the roadway. The regime of the (F-F-F) phase can be obtained by imposing the constraints $\alpha_0 < \beta'$, $\alpha' < \beta''$, and $\alpha'' < \beta_0$. The effective rates can be solved by balancing the flow across the ramp. The analytical expressions are as follows:

$$\alpha' = \frac{\alpha_0(1-\beta_1)}{1+\alpha_0\beta_1} \quad \text{and} \quad \beta' = 1; \tag{9}$$

$$\alpha'' = \alpha' + \alpha_1(1+\alpha') \quad \text{and} \quad \beta'' = \frac{\alpha'(1+\alpha_1)}{\alpha' + \alpha_1(1+\alpha')}. \tag{10}$$

It is interesting to note that the crucial condition is the free flow on the third part of the roadway, i.e., $\alpha'' < \beta_0$, which becomes

$$\alpha_1(1+\alpha_0) - \beta_1(1+\beta_0)\alpha_0 < \beta_0 - \alpha_0. \tag{11}$$

As to the (F-F-J) phase, the effective rates for the on-ramp shown in Eq. (10) should be revised as follows:

$$\alpha'' = \frac{1}{1-\rho^*} \cdot \frac{\beta_0}{1+\beta_0} \quad \text{and} \quad \beta'' = \frac{1}{\rho^*} \cdot \frac{\alpha'}{1+\alpha'}, \tag{12}$$

where ρ^* denotes the average density of the on-ramp, which can be expressed analytically as

$$\rho^* = 1 - \frac{\beta_0}{\alpha_1(1+\beta_0)} + \frac{\alpha'}{\alpha_1(1+\alpha')}. \tag{13}$$

The phase regime can be obtained by the constraints $\alpha_0 < \beta'$, $\alpha' < \beta''$, and $\alpha'' > \beta_0$. The congestion on the third part of the roadway leads to

$$\alpha_1(1+\alpha_0) - \beta_1(1+\beta_0)\alpha_0 > \beta_0 - \alpha_0, \tag{14}$$

while the free flow on the second part of the roadway provides a further constraint as

$$\alpha_1(1+\alpha_0)\beta_0 - \beta_1(1+\beta_0)\alpha_0 < \beta_0 - \alpha_0. \tag{15}$$

These two equations define the boundaries of the (F-F-J) phase. The regimes for the (F-J-J) phase and the (J-J-J) phase can also be obtained similarly. We summarize the results as follows:

$$\text{(F-F-F)} \quad \alpha_1(1+\alpha_0) - \beta_1(1+\beta_0)\alpha_0 < \beta_0 - \alpha_0; \tag{16}$$

$$\text{(F-F-J)} \quad \alpha_1(1+\alpha_0) - \beta_1(1+\beta_0)\alpha_0 > \beta_0 - \alpha_0,$$

$$\alpha_1(1+\alpha_0)\beta_0 - \beta_1(1+\beta_0)\alpha_0 < \beta_0 - \alpha_0; \tag{17}$$

$$\text{(F-J-J)} \quad \alpha_1(1+\alpha_0)\beta_0 - \beta_1(1+\beta_0) < \beta_0 - \alpha_0,$$

$$\alpha_1(1+\alpha_0)\beta_0 - \beta_1(1+\beta_0)\alpha_0 > \beta_0 - \alpha_0; \tag{18}$$

$$\text{(J-J-J)} \quad \alpha_1(1+\alpha_0)\beta_0 - \beta_1(1+\beta_0) > \beta_0 - \alpha_0. \tag{19}$$

The results of a single ramp can be reproduced by setting $\alpha_1=0$ or $\beta_1=0$. We note that the four-dimensional parameter space $(\alpha_0, \beta_0, \alpha_1, \beta_1)$ can be completely classified into these

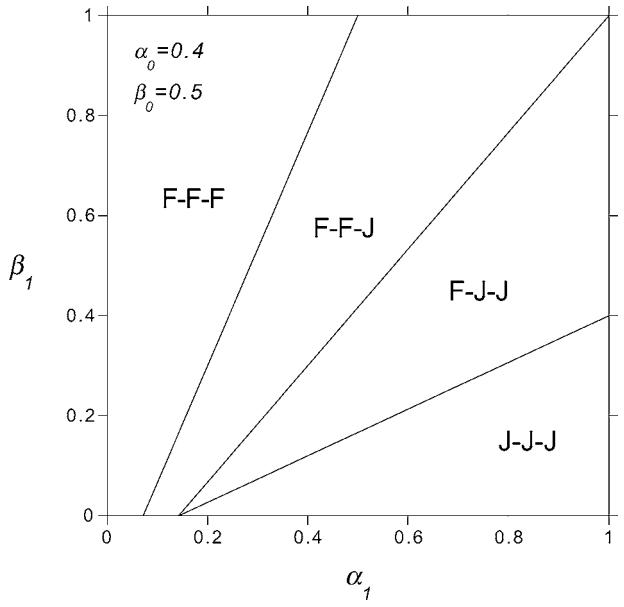

FIG. 2. Phase diagram in the ramp flow (α_1,β_1) for the system shown in Fig. 1(a). The boundary flow is fixed at $(\alpha_0,\beta_0)=(0.4,0.5)$.

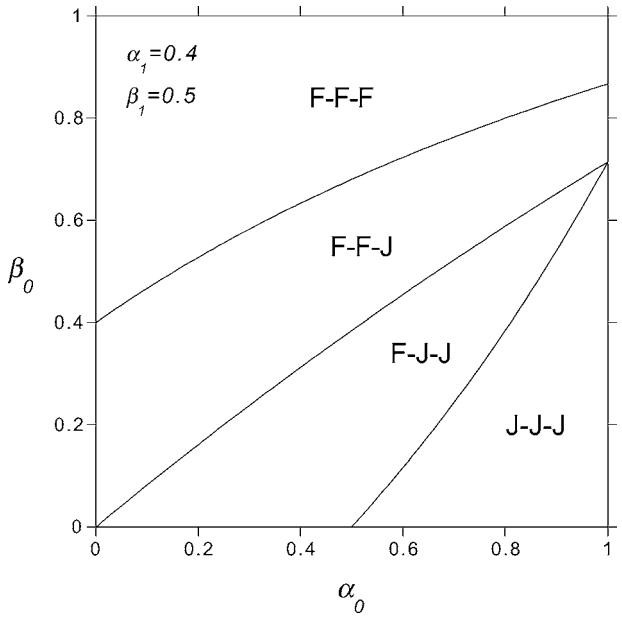

FIG. 3. Phase diagram in the boundary flow (α_0,β_0) for the system shown in Fig. 1(a). The ramp flow is fixed at $(\alpha_1,\beta_1)=(0.4,0.5)$.

four distinct phases. With naive intuition, the two ramps divide the roadway into three sections, and each section can be either free or jam. Thus one would expect eight different phases. However, there are four phases missing: (J-F-F), (J-J-F), (J-F-J), and (F-J-F). Along the traffic direction, free flow will not follow the congestion. With a typical boundary flow (α_0,β_0), the phase diagram in the ramp flow (α_1,β_1) is shown in Fig. 2. All four different phases can be realized by appropriate choices of (α_1,β_1). Basically, the traffic jams emerge as α_1 increases and resolve as β_1 increases. It is interesting to notice that all the phase boundaries on the phase diagram (α_1,β_1) are straight lines. On the other hand, with a typical ramp flow (α_1,β_1), the phase diagram in the boundary flow (α_0,β_0) is shown in Fig. 3. Again, all four different phases can be realized by appropriate choices of (α_0,β_0). The traffic jams appear as α_0 increases and disappear as β_0 increases. The phase boundaries become curved. The numerical simulations can be exactly reproduced (not shown).

III. MAXIMUM FLOW

Next, we switch the order of the two ramps. The on-ramp is now placed before the off-ramp as shown in Fig. 1(b). The flow from the on-ramp α_1 can be taken account of by a removal rate β' for the first part and an injection rate α' for the second part of the roadway; the flow from the off-ramp β_1 can also be taken account of by a removal rate β'' for the second part and an injection rate α'' for the third part of the roadway. In the regime of the (F-F-F) phase, the analytical expressions shown in Eqs. (9) and (10) now become the following:

$$\alpha' = \alpha_0 + \alpha_1(1+\alpha_0) \quad \text{and} \quad \beta' = \frac{\alpha_0(1+\alpha_1)}{\alpha_0 + \alpha_1(1+\alpha_0)}; \tag{20}$$

$$\alpha'' = \frac{\alpha'(1-\beta_1)}{1+\alpha'\beta_1} \quad \text{and} \quad \beta'' = 1. \tag{21}$$

The free flow on the third part of the roadway leads to the constraint

$$\alpha_1(1+\alpha_0) - \beta_1(1+\beta_0)\alpha_0 - \alpha_1\beta_1(1+\alpha_0)(1+\beta_0) < \beta_0 - \alpha_0. \tag{22}$$

In this case, however, the free flow on the first part of the roadway also imposes further constraint as

$$\alpha_1 < \frac{1-\alpha_0}{1+\alpha_0}. \tag{23}$$

Together, the above two equations mark the boundaries of the (F-F-F) phase. Similarly, we summarize the results for the four different phases in the following:

$$\text{(F-F-F)} \quad \alpha_1(1+\alpha_0) - \beta_1(1+\beta_0)\alpha_0 - \alpha_1\beta_1(1+\alpha_0)(1+\beta_0) < \beta_0 - \alpha_0,$$
$$\alpha_1 < \frac{1-\alpha_0}{1+\alpha_0}; \tag{24}$$

$$\text{(F-F-J)} \quad \alpha_1(1+\alpha_0) - \beta_1(1+\beta_0)\alpha_0 - \alpha_1\beta_1(1+\alpha_0)(1+\beta_0) > \beta_0 - \alpha_0,$$
$$\alpha_1(1+\alpha_0) - \beta_1(1+\beta_0) < \beta_0 - \alpha_0; \tag{25}$$

$$\text{(F-J-J)} \quad \alpha_1(1+\alpha_0)\beta_0 - \beta_1(1+\beta_0) + \alpha_1\beta_1(1+\alpha_0)(1+\beta_0) < \beta_0 - \alpha_0,$$

$$\alpha_1(1+\alpha_0)-\beta_1(1+\beta_0)>\beta_0-\alpha_0; \tag{26}$$

$$\text{(J-J-J)}\quad \alpha_1(1+\alpha_0)\beta_0-\beta_1(1+\beta_0)+\alpha_1\beta_1(1+\alpha_0)(1+\beta_0)$$

$$>\beta_0-\alpha_0,$$

$$\beta_1<\frac{1-\beta_0}{1+\beta_0}. \tag{27}$$

Again, the above results reduce correctly to the cases of a single ramp with the setting $\alpha_1=0$ or $\beta_1=0$. It is interesting to notice that the above four phases do not completely classify the parameter space $(\alpha_0,\beta_0,\alpha_1,\beta_1)$. In fact, one more distinct phase can be observed. The traffic flow saturates to the maximum value on the second part of the roadway, while the congestion remains on the first part of the roadway and the free flow is maintained on the third part of the roadway. The phase regime can be obtained as follows:

$$\text{(J-M-F)}\quad \alpha_1>\frac{1-\alpha_0}{1+\alpha_0},$$

$$\beta_1>\frac{1-\beta_0}{1+\beta_0}, \tag{28}$$

where free flow (F), jams (J), and maximum flow (M) can be observed in different parts of the roadway. With these five different phases, the parameter space $(\alpha_0,\beta_0,\alpha_1,\beta_1)$ can then be completely classified. In last section (the off-ramp placed before the on-ramp), the maximum flow can only be observed along the phase boundaries in extreme conditions $\alpha_0=1$ and/or $\beta_0=1$. When the off-ramp is placed after the on-ramp, the maximum flow can be observed in an extended regime and becomes a distinct phase. With a typical boundary flow (α_0,β_0), the phase diagram in the ramp flow (α_1,β_1) is shown in Fig. 4. Basically, the congestion develops as α_1 increases and the free flow restores as β_1 increase. However, when α_1 and β_1 are larger than certain criteria, the traffic flow would saturate in the middle section of the roadway and an interesting phase appears. Similarly, with a typical ramp flow (α_1,β_1), the phase diagram in the boundary flow (α_0,β_0) is shown in Fig. 5. An interesting phase emerges whenever α_0 and β_0 are larger than certain criteria. We emphasize again that the above analytical results are exact. The numerical simulations can be correctly reproduced (not shown).

IV. TRAFFIC ROTARY

When the periodic boundary conditions are imposed, the system configuration shown in Fig. 1 becomes a traffic rotary (see Fig. 6). There are only two control parameters α_1 and β_1. The effective values of α_0 and β_0 can be deduced as following. If one starts with Fig. 1(a), the connected boundaries are in the upper branch (part 1). In the free-flow regime, the flow balance requires $\beta_0=1$ and $\alpha_0=\alpha''$, which can then be used to obtain $\alpha_0=\alpha_1/\beta_1$. The constraint of Eq. (16) becomes $\alpha_1<\beta_1$. The densities in different parts of the rotary can also be obtained:

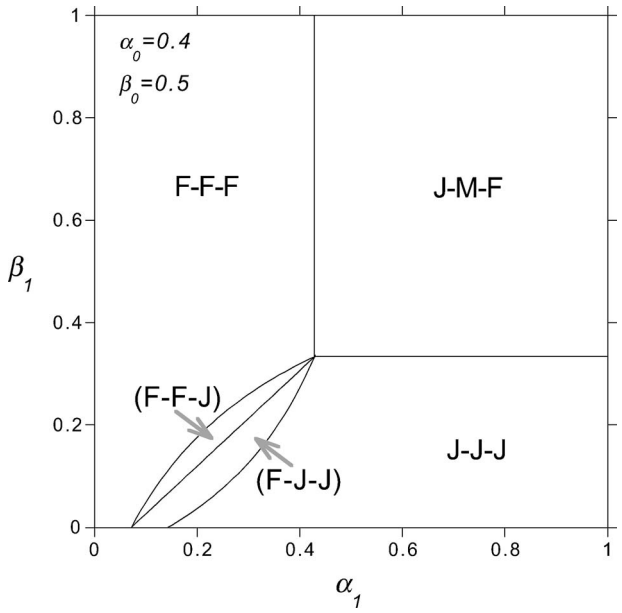

FIG. 4. Same as in Fig. 2. In contrast, the on-ramp is now placed before the off-ramp as shown in Fig. 1(b).

$$\rho_1=\frac{\alpha_1}{\alpha_1+\beta_1}\quad\text{and}\quad\rho_2=\frac{\alpha_1(1-\beta_1)}{\alpha_1+\beta_1}. \tag{29}$$

In the congestion regime, the flow balance requires $\alpha_0=1$ and $\beta_0=\beta'$, which can then be used to obtain $\beta_0=\beta_1/\alpha_1$. The constraint of Eq. (19) becomes $\alpha_1>\beta_1$. The densities in different parts of the rotary become

$$\rho_1=\frac{\alpha_1}{\alpha_1+\beta_1}\quad\text{and}\quad\rho_2=\frac{\alpha_1(1+\beta_1)}{\alpha_1+\beta_1}. \tag{30}$$

To summarize, we obtain only two different phases as follows:

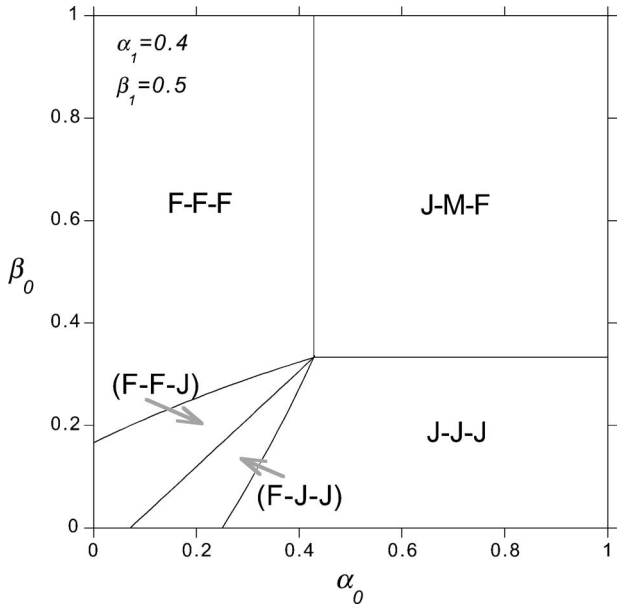

FIG. 5. Same as in Fig. 3. In contrast, the on-ramp is now placed before the off-ramp as shown in Fig. 1(b).

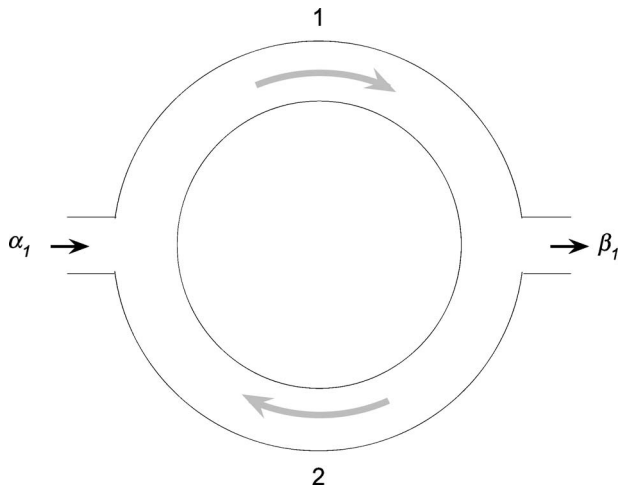

FIG. 6. System configuration of a traffic rotary. Particles move clockwise as shown by the gray arrows. The upper and lower branches are labeled as part 1 and part 2, respectively.

$$\text{(F-F)} \quad \alpha_1 < \beta_1, \tag{31}$$

$$\text{(J-J)} \quad \alpha_1 > \beta_1. \tag{32}$$

When the injection α_1 is less than the removal β_1, the free flow can be observed in both branches; when α_1 is larger than β_1, the congestion dominates in both branches. Since the free flow will not follow the congestion along the traffic direction, both (F-J) and (J-F) phases cannot be realized on a rotary. As α_1 and β_1 vary, ρ_1 changes continuously, while ρ_2 displaces a discontinuity at $\alpha_1=\beta_1$. Right on the phase transition boundary $\alpha_1=\beta_1$, the traffic in the upper branch (part 1) saturates to the maximum and the traffic in the lower branch (part 2) reveals a phase separation. The density in part 1 is homogeneous and assumes a value of $\frac{1}{2}$. In contrast, the density in part 2 is inhomogeneous. Near the on-ramp (α_1), the traffic is congested and the density is $(1+\beta_1)/2$; near the off-ramp (β_1), the free flow is observed and the density is $(1-\beta_1)/2$. We note that the same results can also be reached by analyzing the configuration of Fig. 1(b).

Next, we add one more ramp to the rotary. The system configuration is shown in Fig. 7. After some calculations, we obtain three distinct phases as follows:

$$\text{(F-F-F)} \quad \alpha_1 < \beta_1 + \beta_2 - \beta_1\beta_2, \tag{33}$$

$$\text{(J-J-J)} \quad \alpha_1 > \beta_1 + \beta_2 + \beta_1\beta_2, \tag{34}$$

$$\text{(M-F-J)} \quad \beta_1 + \beta_2 - \beta_1\beta_2 < \alpha_1 < \beta_1 + \beta_2 + \beta_1\beta_2. \tag{35}$$

It is interesting to observe that the free flow (F-F-F) and the congestion (J-J-J) do not completely classify the parameter space $(\alpha_1, \beta_1, \beta_2)$. As the free flow will not follow the congestion, the coexistence of free flow and congestion on a rotary must always involve a phase of maximum flow (M). In such a situation, part 1 of the rotary emerges as a bottleneck to the traffic. Free flow is still maintained in part 2 and congestion is observed in part 3. The typical phase diagrams in (α_1, β_1) and (β_1, β_2) are shown in Figs. 8 and 9, respectively. When the ramp flow is reversed, i.e., the rotary has two on-ramps (α_1, α_2) and one off-ramp (β_1), the parameter space $(\alpha_1, \alpha_2, \beta_1)$ can be classified by the same three phases as follows:

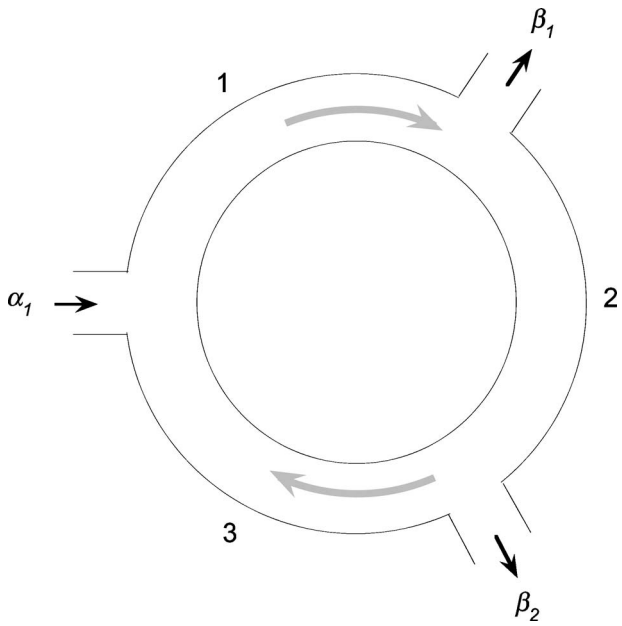

FIG. 7. A rotary with three ramps: one on-ramp (α_1) and two off-ramps (β_1, β_2). The rotary is then divided into three parts labeled by the number.

$$\text{(F-F-F)} \quad \beta_1 > \alpha_1 + \alpha_2 + \alpha_1\alpha_2, \tag{36}$$

$$\text{(J-J-J)} \quad \beta_1 < \alpha_1 + \alpha_2 - \alpha_1\alpha_2, \tag{37}$$

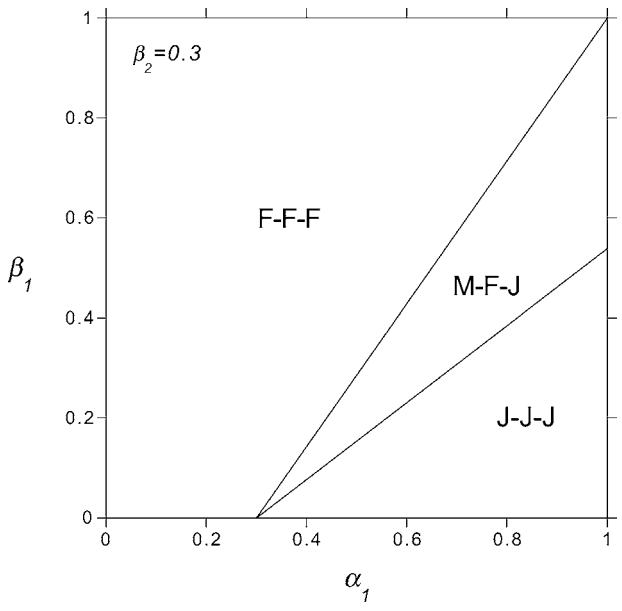

FIG. 8. Phase diagram in the ramp flow (α_1, β_1) for the system shown in Fig. 7. The other ramp flow is fixed at β_2=0.3.

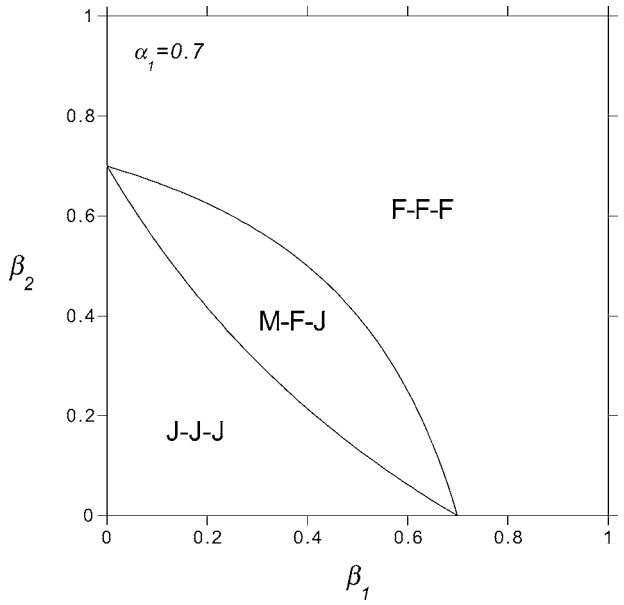

FIG. 9. Phase diagram in the ramp flow (β_1, β_2) for the system shown in Fig. 7. The other ramp flow is fixed at $\alpha_1 = 0.7$.

$$\text{(F-J-M)} \quad \alpha_1 + \alpha_2 - \alpha_1\alpha_2 < \beta_1 < \alpha_1 + \alpha_2 + \alpha_1\alpha_2. \quad (38)$$

The saturated flow always emerges between an on-ramp and an off-ramp, with the on-ramp coming before the off-ramp along the traffic direction.

With two on-ramps and two off-ramps, the rotary shown in Fig. 10 can be taken as an alternative to the conventional crossroad. Traffic from west to east is prescribed by α_1 and β_1; traffic from south to north is prescribed by α_2 and β_2. Besides the free flow (F-F-F-F) and congestion (J-J-J-J), the maximum flow can only be expected in part 1 of the rotary. In such a situation, part 2 will be free flow and part 4 will be congested. Part 3 can be either free or jam. Thus we should

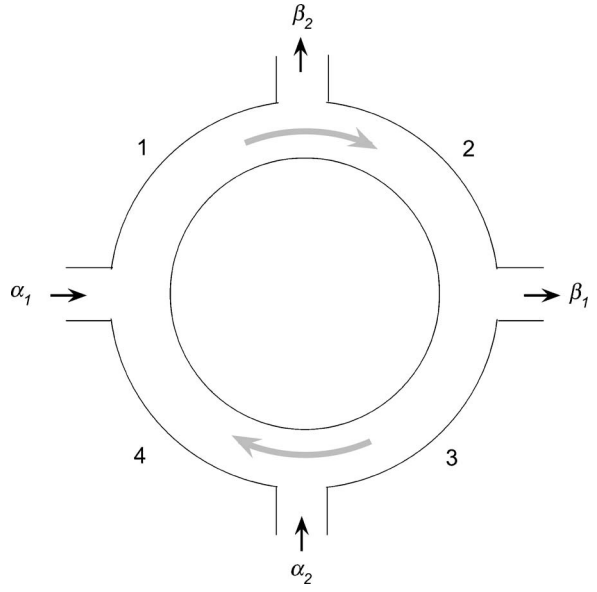

FIG. 10. A traffic rotary with four ramps.

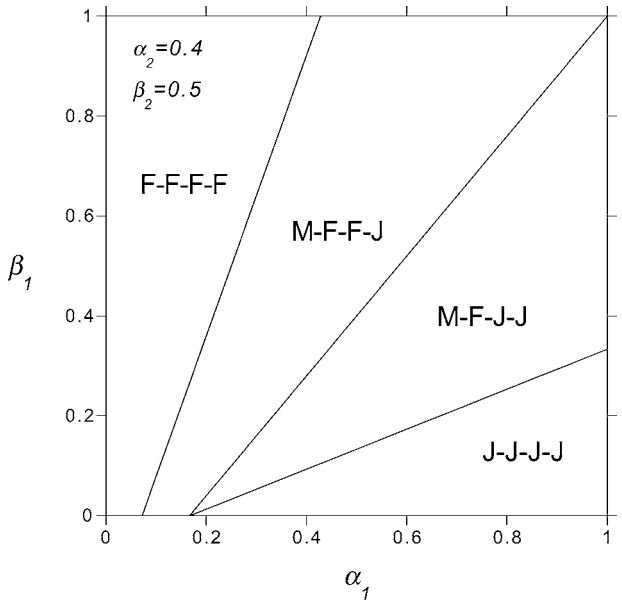

FIG. 11. Phase diagram in the ramp flow (α_1, β_1) for the system shown in Fig. 10. The other ramp flow is fixed at $(\alpha_2, \beta_2) = (0.4, 0.5)$.

have four different phases. The results are as follows:

$$\text{(F-F-F-F)} \quad \alpha_1 + \alpha_2 + \alpha_1\alpha_2 < \beta_1 + \beta_2 - \beta_1\beta_2, \quad (39)$$

$$\text{(J-J-J-J)} \quad \beta_1 + \beta_2 + \beta_1\beta_2 < \alpha_1 + \alpha_2 - \alpha_1\alpha_2, \quad (40)$$

$$\text{(M-F-F-J)} \quad \alpha_1 + \alpha_2 - \alpha_1\alpha_2 < \beta_1 + \beta_2 - \beta_1\beta_2 < \alpha_1 + \alpha_2 + \alpha_1\alpha_2, \quad (41)$$

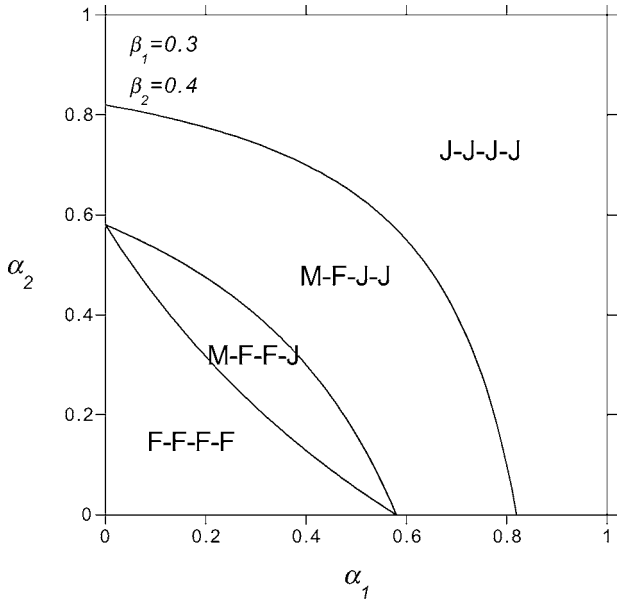

FIG. 12. Phase diagram in the ramp flow (α_1, α_2) for the system shown in Fig. 10. The other ramp flow is fixed at $(\beta_1, \beta_2) = (0.3, 0.4)$.

$$\text{(M-F-J-J)} \quad \beta_1+\beta_2-\beta_1\beta_2<\alpha_1+\alpha_2-\alpha_1\alpha_2 < \beta_1+\beta_2+\beta_1\beta_2. \quad (42)$$

The typical phase diagrams in (α_1,β_1) and (α_1,α_2) are shown in Figs. 11 and 12, respectively. With the above analytical results, other kinds of phase diagrams can also be obtained easily.

V. CONCLUDING REMARKS

In this paper, we study the phase diagrams of asymmetric simple exclusion processes with nontrivial boundaries. We demonstrate that the bulk properties on the roadway are totally controlled by the stochastic ramp-flow through the boundaries. To classify the traffic conditions, the roadway can be divided into various parts joined by the ramps. On each part, the traffic is homogeneous and can be characterized as free flow, congestion, or maximum flow. Complete classification in the parameter space is achieved. Exact phase diagrams are obtained analytically. Basically the traffic jams emerge as the on-ramp flow increases. The free flow is restored as the off-ramp flow increases. In between these two phases, various kinds of inhomogeneity can be developed among different parts of the roadway. Along the traffic direction, we find that the free flow will not follow the congestion directly. To constitute a bottleneck, the maximum flow must appear in between the downstream free-flow and the upstream congestion, which also implies that the on-ramp must be placed before the off-ramp along the traffic direction. In the simple model studied, the present results are exact. These transparent results might be useful to analyze the real traffic network. The bottlenecks on a complex network can then be readily identified. A control scheme to ease the congestion can also be advised.

In this work, the dynamics is deterministic and the symmetry between particle and hole is intact. For more realistic models, the noises shall not be neglected and higher velocities shall be considered. A nature extension is the well-known Nagel-Schreckenberg model [11,12]. The particle-hole symmetry will be broken by higher velocities. As the prominent effects of higher velocities are revealed near the boundaries [13], we expect that similar results in bulk can be reached. However, when the noises are present, a single ramp is more than enough to stabilize the maximum flow. Without noises, at least two ramps are necessary to support the maximum flow. The phase diagram is expected to change dramatically. It would be interesting to further explore the similarity between the stochastic dynamics without a ramp and the deterministic dynamics with two ramps. We also conjecture that, when the noises are included, the effects of higher velocities will further emerge [14].

[1] D. Chowdhury, L. Santen, and A. Schadschneider, Phys. Rep. **319**, 199 (2000).
[2] R. Mahnke, J. Kaupužs, and I. Lubashevsky, Phys. Rep. **408**, 1 (2005).
[3] J. Krug, Phys. Rev. Lett. **67**, 1882 (1991).
[4] C. Appert and L. Santen, Phys. Rev. Lett. **86**, 2498 (2001).
[5] B. Derrida and M. R. Evans, in *Nonequilibrium Statistical Mechanics in One Dimension*, edited by V. Privman (Cambridge University Press, Cambridge, UK, 1997).
[6] B. Derrida, Phys. Rep. **301**, 65 (1998).
[7] B. S. Kerner and H. Rehborn, Phys. Rev. Lett. **79**, 4030 (1997).
[8] D. Helbing and M. Treiber, Phys. Rev. Lett. **81**, 3042 (1998).
[9] H. Y. Lee, H. W. Lee, and D. Kim, Phys. Rev. Lett. **81**, 1130 (1998).
[10] D. W. Huang, Phys. Rev. E **72**, 016102 (2005).
[11] K. Nagel and M. Schreckenberg, J. Phys. I **12**, 2221 (1992).
[12] M. Schreckenberg, A. Schadschneider, K. Nagel, and N. Ito, Phys. Rev. E **51**, 2939 (1995).
[13] D. W. Huang, Phys. Rev. E **63**, 012104 (2001).
[14] D. W. Huang, Phys. Rev. E **64**, 036108 (2001).